Nanoscale

Cite this: *Nanoscale*, 2012, **4**, 7334

www.rsc.org/nanoscale

COMMUNICATION

Functionalized gold magic clusters: $Au_{25}(SPhNH_2)_{17}$†

Christophe Lavenn,[a] Florian Albrieux,[b] Gérard Bergeret,[a] Rodica Chiriac,[c] Pierre Delichère,[a] Alain Tuel[a] and Aude Demessence*[a]

Received 20th August 2012, Accepted 4th October 2012
DOI: 10.1039/c2nr32367b

New Au_{25} nanoclusters stabilized by heterotopic 4-aminothiophenolate ligands ($HSPhNH_2$) have been isolated with a yield of ~70%. The nanoclusters formula determined by ESI-MS is $Au_{25}(SPhNH_2)_{17}$, with the 18th position occupied by an amine or DMF molecules to close their electronic shell.

Atomically well-defined thiolate gold nanoclusters have emerged in recent years as a new class of materials.[1] These sub-2 nm clusters, with the formula $Au_n(SR)_m$, are formed by a precise number n of gold atoms comprised between ~10 and a few hundred and stabilized by m thiolate molecules. What renders uniqueness to these clusters is the discrete electronic structure of the gold core due to quantum size effects, which gives them original properties intermediate between those of molecular and bulk states.[1] As a result they are good model candidates to study, with an atomic precision, various properties such as optics,[2] magnetism[3] and catalysis[4] and also to attempt to understand the size effect in nanotechnology. The formation of well defined $[Au_n(SR)_m]^z$ thiolate clusters follows a nano-scaling law[5] with commonly observed $(n,m)^z$ compositions from $(25,18)^{0/-1}$,[3b,6] (38,24),[7] (68,34),[8] (102,44),[9] (144,60)[10] up to (333,79).[11] The origin of the formation and the high stability of some clusters have been explained by a "superatom concept" which considers that the clusters are stable when their electronic shell is closed and are referred to as magic clusters.[12] This is the case of $(25,18)^-$ (8e), $(44,28)^{2-}$ (18e), (68,34) (34e) and (102,44) (58e) nanoclusters. But among the various spherical clusters, many are stable without conforming to the electron shell closing numbers, including (25,18) (7e) and (144,60) (84e). So the electronic factor is not the only contribution to be taken into account; the geometry has also to be considered to understand the formation and stability of the clusters.[12] From a synthetic point of view, numerous gold clusters have been observed and sometimes purified, however up to now, the main thiolate ligand used is phenylethylthiolate, forming a large quantity of clusters from Au_{10} to Au_{333}.[7,8,11,13] Nanoclusters have also been isolated with glutathione[14] and alkanethiolates,[15] and a few have also been reported with *para*-substituted thiophenol SPhX (X = H, NO_2, Br, CH_3, OCH_3, CO_2H),[1a,9,16] or with functional ligands like pyrene and azobenzene thiolate derivatives.[17] From these observations, it appears that to fully understand the formation of gold clusters, their stability, the electron shell filling and the geometric contribution, extended studies have to be done with various ligands under different synthetic conditions. Moreover to go further in the applications of gold nanoclusters in optics or nanotechnology, functionalized particles have to be developed to be deposited on substrates or coupled with spacers, and more importantly in an easy way and in a high yield. So to study the influence of the ligands on the cluster formation, we propose to use a new thiolate molecule, 4-aminothiophenol. The first advantage of using an aromatic group directly connected to the cluster through a thiolate function is to facilitate the electron transfer between the organic and inorganic parts to target appropriate electronic applications. Secondly, this ligand also brings an amino function at the surface, which makes the nanoclusters promising candidates for functional units or building blocks of novel materials.[18] Among the few nanoclusters made with thiophenol derivatives, only one system has been reported by direct synthesis from chloroauric acid: $Au_{102}(SPhCO_2H)_{44}$.[9,19] Other SPhX ligands (X = H, NO_2, Br, CH_3, OCH_3) have been grafted by ligand exchange reactions starting from $Au_n(SCH_2CH_2Ph)_m$ with (n,m) = (25,18) and (38,24) and keeping the same composition.[1a,16,9] Nevertheless, in the case of the exchange reaction from $Au_{38}(SCH_2CH_2Ph)_{24}$ and thiophenol, the resulting particles are $Au_{36}(SPh)_{23}$.[16c] The loss of two gold atoms and one ligand points out that the formation of thiophenol-based clusters may sometimes not follow the same formula observed with $Au_n(SCH_2CH_2Ph)_m$ and imply structural modifications and formation of new clusters. We report here a surfactant-free and easy one-step synthesis of the first pure Au_{25} clusters with an amino functionalized thiophenol. Surprisingly, this cluster does not follow the common formula $Au_{25}(SR)_{18}$ but forms an extended network $Au_{25}(SPhNH_2)_{17}$ through amino–gold interactions. In that configuration, this cluster has 8 valence electrons and a closed electronic structure, which explains its stability. Here we present the synthesis, characterizations and optics of this new magic cluster.

In a typical synthesis (see ESI† for details), two distinct solutions of $LiBH_4$ and $HAuCl_4$ in THF are simultaneously added dropwise, over

[a]*Institut de Recherches sur la Catalyse et l'Environnement de Lyon (IRCELYON), UMR 5256 CNRS-Université Lyon 1, 2 avenue Albert Einstein, 69626 Villeurbanne, France. E-mail: aude.demessence@ircelyon.univ-lyon1.fr; Tel: +33 472 445 322*
[b]*Centre Commun de Spectrométrie de Masse, UMR 5246 CNRS-Université Lyon 1, 43 Boulevard du 11 Novembre 1918, 69622 Villeurbanne, France*
[c]*Laboratoire des Multimatériaux et Interfaces (LMI), UMR 5615 CNRS-Université Lyon 1, 43 Boulevard du 11 Novembre 1918, 69622 Villeurbanne, France*

† Electronic supplementary information (ESI) available: Synthesis of nanoclusters, ESI-MS, TGA, elemental analysis, XPS, PXRD, FT-IR, and MET experiments. See DOI: 10.1039/c2nr32367b

a period of ~30 minutes, to a stirred solution of 4-aminothiophenol in THF at room temperature. The formation of gold clusters was allowed to proceed for five hours. THF is then removed by rotary evaporation and the nanoclusters are thoroughly precipitated and washed with an excess of ethanol.

The so-obtained product is poorly dispersible in almost all solvents except *N*,*N*-dimethylformamide (DMF). The average yield obtained is 70% and all following characterizations are done without further purifications. This one-pot synthesis, without the use of size-exclusion chromatography, the absence of a surfactant and the high yield producing around 100 mg of clusters, is really interesting for further applications.

To establish the (*n*,*m*) ratio in the formula $Au_n(SR)_m$ and also to check the purity of the products, mass spectrometry (MS) is the technique of choice. Electro-spray ionization mass spectrometry (ESI-MS) has been employed because it is known to be a soft ionization technique that does not usually imply nanoclusters fragmentation.[20] An ESI-MS spectrum of the sample dispersed in a mixture containing DMF (Fig. 1) shows a dominant peak at $m/z = 3517.2510$ Th, corresponding to the doubly charged $Au_{25}(SPhNH_2)_{17}$ clusters. The isotope pattern of $Au_{25}(SPhNH_2)_{17}$ matches perfectly with the simulated spectra with an error of 4.5 ppm and a resolving power of 15 000. The good signal obtained for the high resolution mass spectrum, without the addition of CsOAc as it is usually done to enhance the cluster ionization, is due to the amino groups which are easily charged compared to unfunctionalized phenyl groups. The whole mass spectrum is quite clean, even if peaks corresponding to $Au_n(SPhNH_2)_m$ with (*n*,*m*) = (25,18), (25,16), (24,16), (23,15) and (22,14) are observed in small quantities. These clusters, thermodynamically unstable, may be present as impurities in the solution or may be formed under the ionization process. Because the number of thiolate ligands, 17, on Au_{25} clusters does not follow the expected $Au_{25}(SR)_{18}$ cluster formula usually found with thiolate derivatives and that $Au_{25}(SPhNH_2)_{18}$ is also observed as a minor peak in Fig. 1, further ESI-MS experiments have been done to confirm the (25,17) ratio. Firstly, no fragment was observed for $Au_{25}(SCH_2CH_2Ph)_{18}$ under the same experimental conditions (Fig. S1 and S2†), meaning that the peaks in the mass spectrum are not considered as fragments

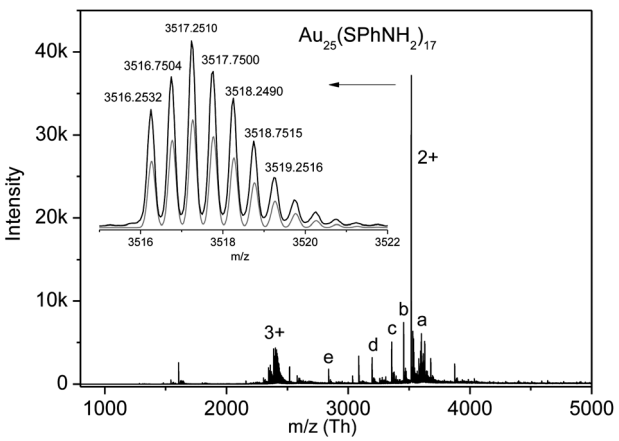

Fig. 1 Positive-ion ESI mass spectrum of $Au_{25}(SPhNH_2)_{17}$ nanoclusters. Inset: isotopic pattern of the peak at $m/z = 3516.2532$ Th and its simulated spectrum in grey ($m/z_{theoretical} = 3516.2691$ Th, error = −4.5 ppm). Peaks from a to e correspond to $Au_n(SPhNH_2)_m$ with (*n*,*m*) = (25,18), (25,16), (24,16), (23,15) and (22,14), respectively.

produced by the ionization process. Secondly, because the stability of $Au_{25}(SCH_2CH_2Ph)_{18}$ and $Au_{25}(SPhNH_2)_{17}$ may not be the same during the ionization process, we carried out several ESI-MS experiments under gentle conditions. Some ESI-MS experiments have been done at lower collision energy from 5 to 100 eV; the resulting spectra obtained in this energy area are all the same, pointing out the stability of the clusters. In addition, the temperature of the ionization of the solution was tested at 200, 150 and 80 °C; again all the resulting spectra are similar, corroborating the existence of $Au_{25}(SPhNH_2)_{17}$ in the solution. We also carried out some cryospray MS; in that case, the more intense peak was still (25,17) with a small percentage of (25,18). Moreover, to check the stability of (25,18) clusters observed as a small peak in the mass spectrum, we increased the collision energy to induce its fragmentation, but we did not see any fragmentation, showing again that (25,17) is not coming from the fragmentation of (25,18) but is present in the solution. In addition thermogravimetric (TGA) and elemental analyses, and also X-ray photoelectron spectroscopy confirm this formula. On the TGA curve (Fig. S3†) the organic weight loss from 150 to 800 °C is 30.4%, which agrees with the expected value (30.0 wt%). Elemental analysis on Au, C, H, S and N gave a S/Au ratio of 0.66 and N/Au ratio of 0.67, which is close to the expected value (17/25 = 0.68) (Table S1†). The absence of chlorides or other halides as counter anions is confirmed by XPS analysis of the nanoclusters meaning that the charge of the clusters is neutral (Fig. S4†). Elemental quantification with XPS gave an S/Au atomic ratio of 0.56 and N/Au atomic ratio of 0.57, in good accordance with the proposed formula.

To check the purity of a whole sample in the solid state, it is also of paramount importance to carry out powder X-ray diffraction. Indeed, this routine technique brings two relevant structural changes: firstly, on the size of the gold core at wide angle XR scattering and secondly, on the interparticle packing distance at small angle XR scattering. Fig. 2 presents the experimental XRD pattern for $Au_{25}(SPhNH_2)_{17}$ at wide and small angle XR scattering; a representation of the whole diagram is displayed in Fig. S5.† At wide angle XR scattering (Fig. 2a), the powder pattern of $Au_{25}(SPhNH_2)_{17}$ is compared to the experimental one of $Au_{25}(SCH_2CH_2Ph)_{18}$ (whole pattern on Fig. S6†) and the theoretical pattern of an isolated Au_{25} cluster calculated by the Debye formula from the crystal data of $Au_{25}(SCH_2CH_2Ph)_{18}$.[21] The good matching of the $Au_{25}(SPhNH_2)_{17}$ pattern with the peaks at $2\theta \approx 38$ and 65° of the experimental and calculated patterns of $Au_{25}(SCH_2CH_2Ph)_{18}$ confirms that the gold core is made of 25 atoms. Indeed the shape and the positions of the diffraction peaks in this area are sensitive to the number of gold atoms forming the gold clusters.[13b,c] To confirm this, we applied the Scherrer model on the peak at around 38° of the three curves, and obtained a gold core diameter of 0.93, 0.91 and 0.87 nm for $Au_{25}(SPhNH_2)_{17}$, experimental and theoretical patterns of $Au_{25}(SCH_2CH_2Ph)_{18}$, respectively.[21b] From the crystal data of $Au_{25}(SCH_2CH_2Ph)_{18}$, the core diameter of Au_{25} is 0.98 nm using the centroid–centroid diameter of the outermost gold atoms, which is in good accordance with the above estimations.[22] This method shows that it is possible to apply the Scherrer model on the large diffraction peak at 38° to obtain an approximation of the number of Au atoms in the isolated cluster, although we should be aware that several diffraction peaks are taken into account. The peak at small angle XR scattering (Fig. 2b) has only been observed for thiolate gold nanoclusters $Au_{144}(SCH_2CH_2Ph)_{60}$, but has never been taken into precise consideration.[13b] In fact, this peak is attributed to a short ordering of

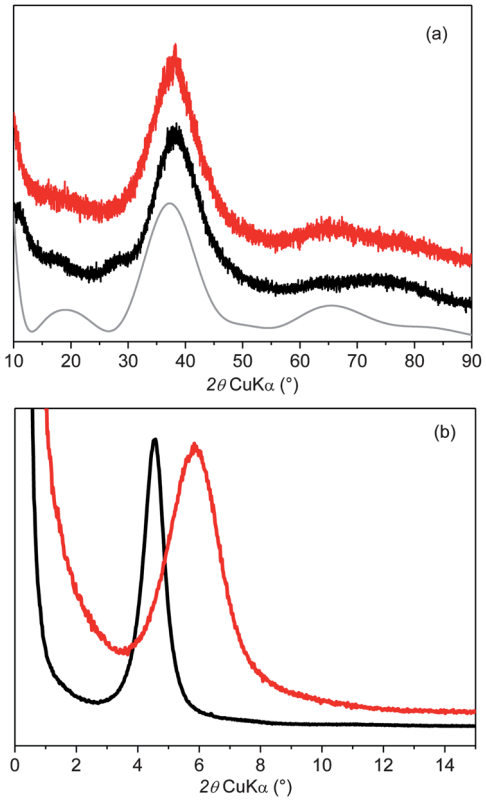

Fig. 2 Experimental PXRD patterns of $Au_{25}(SPhNH_2)_{17}$ (red) and $Au_{25}(SCH_2CH_2Ph)_{18}$ (black) compared to the calculated XRD pattern of an isolated Au_{25} cluster (grey) (a) at wide angle and (b) at small angle.

the clusters, related to the interparticle distance. Moreover, when this peak is fine and intense, this means that the clusters are homogeneous in size and the position of the peak gives the center-to-center particle distance by Bragg's law. The distance is 1.95 and 1.51 nm for $Au_{25}(SCH_2CH_2Ph)_{18}$ and $Au_{25}(SPhNH_2)_{17}$, respectively, which gives an interparticle distance of 0.97 and 0.53 nm (based on an Au_{25} core of 0.98 nm). For $Au_{25}(SCH_2CH_2Ph)_{18}$, this value is in good accordance with the ligand length (0.7 nm), which means that there are two layers of thiolate molecules with a certain interpenetration as it is observed in the crystal structure. In the case of $Au_{25}(SPhNH_2)_{17}$ the short interparticle distance matches with the length of one ligand (0.6 nm), which means that some aminothiophenol molecules are bridging the gold nanoclusters. From this observation coupled with the formula determined by ESI-MS, we propose that two ligands per clusters are connecting the particles making a network with a formula $\{Au_{25}(\mu\text{-}SPhNH_2)_{16.5}(\mu\text{-}NH_2PhS)_{0.5}\}_x$. In this configuration, gold clusters are surrounded by 17 thiolate functions and one amino group, keeping the $Au_{25}(SR)_{18}$ structure and filling their electron shell to get a stable magic cluster.

Fig. 3 shows the high resolution photoelectron spectra of $Au_{25}(SPhNH_2)_{17}$ from Au_{4f} and N_{1s}. The $4f_{7/2}$ and $4f_{5/2}$ binding energies of gold (Fig. 3a) are at 84.7 and 88.4 eV, respectively; these fine peaks with a FWHM of 1.1 eV suggest that there is only one gold state in the clusters. The $4f_{7/2}$ BE peak is really close to the reported $Au_{25}(SR)_{18}$ nanoclusters, for example, the one with SR = glutathione is at 84.8 eV.[23] Compared to bigger functionalized $SPhNH_2$ particles of *ca.* 3 nm (84.2 eV), a positive shift of 0.5 eV for the $4f_{7/2}$ BE peak, from bigger particles to smaller, is observed and is attributed to the

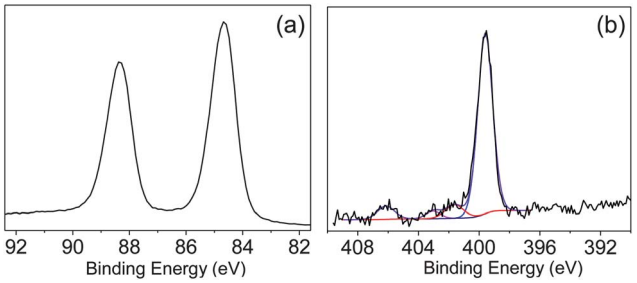

Fig. 3 XPS analysis of $Au_{25}(SPhNH_2)_{17}$ nanoclusters, (a) from Au_{4f} and (b) from N_{1s} (black). The colored lines are the deconvoluted individual peaks of different species present in the sample.

core reduction.[24] The N 1s region was also examined, and is given in Fig. 3b. The peak of N1s at 399.6 eV is assigned to free amino groups, which are the main part of the cluster (measured 83% and expected 97%). Moreover, the additional peak at 401.6 eV is assigned to the interaction of the amine groups with gold (measured 7% and expected 3%), which proves that some ligands are bridging the clusters.[25] Note that the presence of peaks at 403.0 and 406.1 eV may be due to oxidation of $-NH_2$ groups (measured 10%). The high resolution S 2p signal of the clusters was also measured, and data are given in ESI (Fig. S7†). The S 2p binding energy occurring at 163.2 eV is typical of thiolated ligands (~163.2 to 163.4 eV)[13c,23] and more importantly shows that the sulfur atoms are not oxidized. Infra-red spectroscopy (Fig. S8†) also confirms that all the thiolate groups are coordinated to gold clusters with the disappearance of the S–H stretching vibration band observed at 2550 cm^{-1} in the free ligand.

The TEM image of $Au_{25}(SPhNH_2)_{17}$ clusters dispersed in DMF shows particles of less than 1 nm (average size 0.8 ± 0.3 nm) (Fig. S9 and S10†). However, when the sample is prepared in ethanol, the clusters form densely packed aggregates of more than 500 nm (Fig. S11†). These highly packed aggregates are also confirmed by nitrogen adsorption carried out at 77 K on the solid sample (Fig. S12†), where no micropores between the particles are observed.

The absorbance spectrum of $Au_{25}(SPhNH_2)_{17}$ dispersed in DMF (Fig. 4) displays a step-like structure characteristic of a discrete electronic structure that is typical of atomically well defined gold nanoclusters.[13a,16c,26] The absorbance peaks at 470 nm (2.64 eV) and at 710 nm (1.75 eV) are red shifted compared to the peak positions of

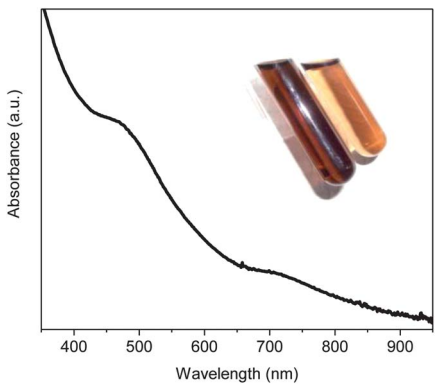

Fig. 4 UV-vis spectrum of $Au_{25}(SPhNH_2)_{17}$ measured in DMF. The inset shows a photograph of the nanoclusters in DMF at different concentrations.

the $Au_{25}(SCH_2CH_2Ph)_{18}$ analog, which are at 400, 450 and 670 nm.[21a] This red shift was already observed when exchanging phenylethylthiolate ligands with substituted thiophenol molecules.[16a] The optical energy gap, $E_g \sim 1.2$ eV (determined from the peak at 1.75 eV), is close to the reported Au_{25} nanoclusters ($E_g \sim 1.3$ eV) and confirms earlier reports that the HOMO–LUMO gap is a signature mark of the gold core and is independent of the type of thiolate molecules at the surface.[13a,16b]

To conclude, $Au_{25}(SPhNH_2)_{17}$ is the first atomically well defined gold nanocluster with the heterotopic 4-aminothiophenol ligand. Its synthesis is a one-step reaction with a yield of ~70%. This cluster adopts an unusual (25,17) *vs.* $(25,18)^{0/-1}$ ratio, and in that configuration, the number of valence electrons being 8, its electronic structure is closed. The formation of this magic cluster is due to the amino group which can occupy the 18th position of the cluster to satisfy the $Au_{25}(SR)_{18}$ structure and without bringing additional charge. In the solid state, $Au_{25}(SPhNH_2)_{17}$ forms a network of coupled gold nanoclusters through organic linkers. In DMF solution, this network disassembles and the amino–gold interaction is replaced by a DMF molecule. These results show the richness of gold thiolate clusters and the ligand effect on their structure. Extended studies with different experimental conditions (privileging direct synthesis) and various thiolate molecules have to be tested to discover original clusters. Theoretical calculations may be helpful to fully understand the arrangement of the ligands at the surface of the clusters and to visualize the packing of the clusters. Well defined $Au_{25}(SPhNH_2)_{17}$ is really appealing for further experiments, because firstly, it brings thiophenol moieties directly coordinated to the clusters, thus providing π electron delocalization for optics and electronics and secondly, it offers possibilities of post-functionalization or deposition on substrates by coupling with the amino groups.

Acknowledgements

CL thanks the French ministry for his PhD grant. M. Aouine and L. Burel are thanked for their help in TEM experiments and N. Cristin and P. Mascunan for elemental analysis.

Notes and references

1 (*a*) J. F. Parker, C. A. Fields-Zinna and R. W. Murray, *Acc. Chem. Res.*, 2010, **43**, 1289; (*b*) R. C. Jin, Y. Zhu and H. Qian, *Chem.–Eur. J.*, 2011, **17**, 6584; (*c*) T. Tsukuda, *Bull. Chem. Soc. Jpn.*, 2012, **85**, 151.
2 I. Dolamic, S. Knoppe, A. Dass and T. Burgi, *Nat. Commun.*, 2012, **3**, 798.
3 (*a*) Y. Negishi, H. Tsunoyama, M. Suzuki, N. Kawamura, M. M. Matsushita, K. Maruyama, T. Sugawara, T. Yokoyama and T. Tsukuda, *J. Am. Chem. Soc.*, 2006, **128**, 12034; (*b*) M. Z. Zhu, C. M. Aikens, M. P. Hendrich, R. Gupta, H. F. Qian, G. C. Schatz and R. C. Jin, *J. Am. Chem. Soc.*, 2009, **131**, 2490.
4 (*a*) Y. Zhu, H. F. Qian, M. Z. Zhu and R. C. Jin, *Adv. Mater.*, 2010, **22**, 1915; (*b*) Y. M. Liu, H. Tsunoyama, T. Akita and T. Tsukuda, *Chem. Commun.*, 2010, **46**, 550.
5 A. Dass, *Nanoscale*, 2012, **4**, 2260.
6 J. Akola, M. Walter, R. L. Whetten, H. Hakkinen and H. Gronbeck, *J. Am. Chem. Soc.*, 2008, **130**, 3756.
7 H. Qian, W. T. Eckenhoff, Y. Zhu, T. Pintauer and R. Jin, *J. Am. Chem. Soc.*, 2010, **132**, 8280.
8 A. Dass, *J. Am. Chem. Soc.*, 2009, **131**, 11666.
9 P. D. Jadzinsky, G. Calero, C. J. Ackerson, D. A. Bushnell and R. D. Kornberg, *Science*, 2007, **318**, 430.
10 O. Lopez-Acevedo, J. Akola, R. L. Whetten, H. Gronbeck and H. Hakkinen, *J. Phys. Chem. C*, 2009, **113**, 5035.
11 H. F. Qian, Y. Zhu and R. C. Jin, *Proc. Natl. Acad. Sci. U. S. A.*, 2012, **109**, 696.
12 M. Walter, J. Akola, O. Lopez-Acevedo, P. D. Jadzinsky, G. Calero, C. J. Ackerson, R. L. Whetten, H. Groenbeck and H. Hakkinen, *Proc. Natl. Acad. Sci. U. S. A.*, 2008, **105**, 9157.
13 (*a*) M. Zhu, C. M. Aikens, F. J. Hollander, G. C. Schatz and R. Jin, *J. Am. Chem. Soc.*, 2008, **130**, 5883; (*b*) H. F. Qian and R. C. Jin, *Nano Lett.*, 2009, **9**, 4083; (*c*) Z. K. Wu, M. A. MacDonald, J. Chen, P. Zhang and R. C. Jin, *J. Am. Chem. Soc.*, 2011, **133**, 9670.
14 (*a*) Y. Shichibu, Y. Negishi, T. Tsukuda and T. Teranishi, *J. Am. Chem. Soc.*, 2005, **127**, 13464; (*b*) Y. Negishi, K. Nobusada and T. Tsukuda, *J. Am. Chem. Soc.*, 2005, **127**, 5261.
15 (*a*) H. F. Qian, M. Z. Zhu, U. N. Andersen and R. C. Jin, *J. Phys. Chem. A*, 2009, **113**, 4281; (*b*) Y. Negishi, C. Sakamoto, T. Ohyama and T. Tsukuda, *J. Phys. Chem. Lett.*, 2012, **3**, 1624.
16 (*a*) R. Guo and R. W. Murray, *J. Am. Chem. Soc.*, 2005, **127**, 12140; (*b*) J. F. Parker, K. A. Kacprzak, O. Lopez-Acevedo, H. Hakkinen and R. W. Murray, *J. Phys. Chem. C*, 2010, **114**, 8276; (*c*) P. R. Nimmala and A. Dass, *J. Am. Chem. Soc.*, 2011, **133**, 9175.
17 (*a*) M. S. Devadas, K. Kwak, J. W. Park, J. H. Choi, C. H. Jun, E. Sinn, G. Ramakrishna and D. Lee, *J. Phys. Chem. Lett.*, 2010, **1**, 1497; (*b*) Y. Negishi, U. Kamimura, M. Ide and M. Hirayama, *Nanoscale*, 2012, **4**, 4263.
18 (*a*) A. P. Tuan, B. C. Choi, K. T. Lim and Y. T. Jeong, *Appl. Surf. Sci.*, 2011, **257**, 3350; (*b*) R. J. Macfarlane, B. Lee, M. R. Jones, N. Harris, G. C. Schatz and C. A. Mirkin, *Science*, 2011, **334**, 204.
19 Y. Levi-Kalisman, P. D. Jadzinsky, N. Kalisman, H. Tsunoyama, T. Tsukuda, D. A. Bushnell and R. D. Kornberg, *J. Am. Chem. Soc.*, 2011, **133**, 2976.
20 (*a*) N. K. Chaki, Y. Negishi, H. Tsunoyama, Y. Shichibu and T. Tsukuda, *J. Am. Chem. Soc.*, 2008, **130**, 8608; (*b*) C. A. Fields-Zinna, J. S. Sampson, M. C. Crowe, J. B. Tracy, J. F. Parker, A. M. deNey, D. C. Muddiman and R. W. Murray, *J. Am. Chem. Soc.*, 2009, **131**, 13844.
21 (*a*) M. Z. Zhu, W. T. Eckenhoff, T. Pintauer and R. C. Jin, *J. Phys. Chem. C*, 2008, **112**, 14221; (*b*) R. E. Dinnebier; S. J. L. Billinge. *Powder Diffraction, Theory and Practice*, RSC Publishing, Cambridge, 2008.
22 M. W. Heaven, A. Dass, P. S. White, K. M. Holt and R. W. Murray, *J. Am. Chem. Soc.*, 2008, **130**, 3754.
23 E. S. Shibu, B. Radha, P. K. Verma, P. Bhyrappa, G. U. Kulkarni, S. K. Pal and T. Pradeep, *ACS Appl. Mater. Interfaces*, 2009, **1**, 2199.
24 J. Sharma, S. Mahima, B. A. Kakade, R. Pasricha, A. B. Mandale and K. Vijayamohanan, *J. Phys. Chem. B*, 2004, **108**, 13280.
25 M. Aslam, L. Fu, M. Su, K. Vijayamohanan and V. P. Dravid, *J. Mater. Chem.*, 2004, **14**, 1795.
26 Y. Shichibu, Y. Negishi, H. Tsunoyama, M. Kanehara, T. Teranishi and T. Tsukuda, *Small*, 2007, **3**, 835.